The persistence and crystallization behavior of atorvastatin calcium amorphous dispersions in polyvinylpyrrolidone

Chaima Tizaoui, Haykel Galai, Simon Clevers, Nicolas Couvrat, Gérard Coquerel, Ivo Rietveld

Version of Record: https://www.sciencedirect.com/science/article/pii/S1773224722002854
Manuscript_22892ee75c3dee4b6243823ad1d200e6

The persistence and crystallization behavior of atorvastatin calcium amorphous dispersions in polyvinylpyrrolidone

Chaima Tizaoui,[a,b,c] Haykel Galai,[b] Simon Clevers,[a] Nicolas Couvrat,[a] Gérard Coquerel,[a] Ivo B. Rietveld[a,d,*]

[a]SMS laboratory (EA 3233), Université de Rouen-Normandie, Place Émile Blondel, 76821 Mont Saint Aignan, France

[b] Laboratoire des matériaux, traitement et analyse (LMTA), Institut national de recherche et d'analyse physico-chimique, Technopole sidi Thabet, 2020 Ariana, Tunisie.

[c] Faculté des sciences de bizerte, University of Carthage, 7021 Zarzouna Bizerte, Tunisia.

[d] Faculté de Pharmacie, Université Paris Cité, 4 avenue de l'observatoire, 75006 Paris, France.

* Corresponding author: ivo.rietveld@univ-rouen.fr

Abstract

The persistence of amorphous atorvastatin calcium has been studied as a function of the amorphization method, polymer content, and relative humidity during storage. For amorphization, ball milling, freeze drying, and spray drying have been used. Polyvinylpyrrolidone K40 (PVP) was mixed with atorvastatin in a wide range of concentrations and the resulting amorphous dispersions were subjected to storage conditions with different levels of relative humidity. The analysis of the glass transition temperature of the various samples demonstrates that interactions between atorvastatin calcium and PVP are unfavorable, leading to a destabilization of amorphous atorvastatin, which becomes therefore more prone to recrystallization. However, mixtures made with spray drying in methanol show an increased glass transition temperature and an increased stability against recrystallisation. PVP may act as a humidity reservoir providing water molecules to amorphous atorvastatin calcium and thus promoting crystallization of the hydrate form. For atorvastatin calcium, the most persistent amorphous sample appears to be that without PVP. It possesses a glass transition temperature as high as 143 °C and it remains amorphous for at least a year independent of the humidity level it is subjected to.

Keywords: Lipitor, atorvastatin calcium, amorphous molecular dispersions, glass transition, hydrate, recrystallisation kinetics

1 Introduction

The stability of drug formulations is an important requirement before market authorization, and it is therefore essential that the stability behavior is thoroughly studied during development (Variankaval, Cote, et Doherty 2008). Nowadays, many active pharmaceutical ingredients are developed using computational methods in which mainly the interactions between the active ingredient and its target are considered. As a result, the best performing active ingredient candidates are generally not very soluble, because this is not a primary selection criterion. To enhance solubilization (or in other words increase the 'apparent solubility'), one approach is to use amorphous drug; however, this increases thermodynamic instability in the formulation leading to a risk of crystallization, which, in turn, may result in practically insoluble drugs. Amorphous drug formulations can be stabilized by dispersing the active pharmaceutical ingredient (API) at the molecular level in an amorphous polymer matrix to limit the mobility of the drug molecules. Kinetic stability of such formulations is ensured through high glass temperatures of the polymer and through interactions between the polymer and the APIs. Even for APIs with high glass transition temperatures, the risk of crystallization from the glassy state at temperatures below the glass transition temperature may be present (Newman et Zografi 2020) for example due to the so-called plastifying effect of water (Rumondor et al. 2009).

Atorvastatin is a synthetic pharmaceutical active ingredient with cholesterol-lowering properties. It belongs to a group of drugs called statins and its trade name is Lipitor (Parke Davis, 2009; Desager et Horsmans 1996). Atorvastatin is used to treat high cholesterol levels. It may also be used for the primary prevention of cardiovascular disease (Colhoun et al., 2004; Pasceri et al., 2004). It reversibly inhibits 3-hydroxy-3-methylglutaryl coenzyme A (HMG-CoA) reductase, which plays a key role in the production of cholesterol in the body (Desager et Horsmans 1996).

The crystalline form of atorvastatin calcium (ATC) is hydrated and at room temperature under a relative humidity of about 50%, it contains three water molecules (Briggs et al., 1997). On increasing the temperature, the water molecules gradually leave the crystal causing a collapse of the structure that is completed at circa 140 °C (Tizaoui et al. 2020; Christensen et al. 2013). ATC is a class II drug according to the Biopharmaceutical Classification System (BCS) (Löbenberg et Amidon 2000; Lau et al. 2006), and its solubility and rate of dissolution from the crystalline state is low (Choudhary et al. 2012; Kasim et al., 2004), limiting oral absorption of ATC.

In order to improve the apparent solubility and dissolution rate of atorvastatin, several processes have been proposed in the literature to obtain amorphous states including spray-drying (Kim et al. 2008), supercritical anti-solvent precipitation (Won et al. 2005; Zhang et al. 2009), complexation with cyclodextrins (Taksande Jayshree B et al. 2017; Zhen-Hai Zhang, Jian-Ping Zhou, Hui-Xia Ly, et al. 2012), nanosuspensions (Arunkumar et al., 2009) and molecular dispersions in amorphous polymers (Sinha et al. 2010; Bobe et al. 2011; Choudhary et al. 2012; Lemsi et al. 2017). Different polymeric substrates, such as cellulosic polymers (M.- S. Kim et al. 2013), polyvinylpyrrolidone - PVP (Bobe et al. 2011; Hu et al. 2014), Poloxamer (Dong et al. 2018; Bhumika Sharma et al. 2012), polyethylene glycol (Bobe et al. 2011; Hu et al. 2014; Maurya, Belgamwar, et Tekade 2010), Eudragit (Kumar et al. 2017; Bobe et al. 2011), and Soluplus (Ha et al. 2014), have been used to prepare solid formulations with increased

dissolution rate using different manufacturing processes. Solid dispersions are attractive for improving the dissolution behavior of poorly water-soluble drugs, because the presence of other components, mainly polymers, generally guarantees relatively high activation energies for recrystallisation. Solid dispersions have improved the solubility and the oral bioavailability of poorly water-soluble drugs such as ibuprofen (Newa et al. 2007), carbamazepine (Zerrouk et al. 2001), naproxen (Adibkia et al. 2013), and ritonavir (Law et al. 2004).

The majority of the publications on solid dispersions demonstrate improved dissolution compared to untreated ATC crystals. Choudhary et al. reported a nearly 33-fold increase in 'apparent solubility' compared to crystalline ATC (Choudhary et al. 2012). Kim et al. showed with amorphous atorvastatin obtained through spray drying that the dissolution rate increased 3.5 times compared to the crystalline form (Kim et al. 2008). Hai-Xia showed that about 89% of the amorphous atorvastatin obtained through antisolvent precipitation was dissolved after 60 minutes, compared to 74% of untreated crystalline atorvastatin (Zhang et al. 2009). Shamsuddin et al. showed a dissolution rate improvement of an ATC formulation with PEG 4000 of about 2 times higher than ATC alone or the corresponding physical mixture (Shamsuddin et al. 2016)). Hu et al. showed that nearly 95% of the ATC in the ATC-PVP K30 solid dispersion dissolved within 5 minutes (Hu et al. 2014). Although increased dissolution alone does not guarantee improved absorption, Sinha et al. has shown that ATC solid dispersions containing polyvinylpyrrolidone (PVP) exhibit a significant increase in absorption of ATC after oral administration (Sinha et al., 2010).

Previous research on ATC mainly describes the amorphous form and its mode of obtention with a focus on formulation, pharmacology, and pharmacokinetics without addressing more generally the stability behavior of this solid amorphous formulation. In the present paper, the kinetic stability of amorphous atorvastatin calcium samples obtained by grinding, freeze drying, or spray-drying has been studied. A comparison of the physicochemical properties of the pure amorphous drug and of mixtures with PVP has been carried out. All samples have been characterized directly after preparation and have then been followed for one year under relative humidity conditions of 0, 57.6 %, 84%, or 98% RH. The effects of PVP, of the preparation method, and of the relative humidity on the stability of amorphous ATC have been evaluated using differential scanning calorimetry (DSC), powder X-ray diffractometry (PXRD), and second harmonic generation spectroscopy (SHG).

2 Materials and methods

2.1 Materials

Crystalline atorvastatin calcium (ATC) trihydrate with a molar weight of 1209.39 g mol^{-1} and polyvinylpyrrolidone K-40 (PVP K40) with an average molar weight of 40000 g mol^{-1} were provided by the National Drug Control Laboratory (LNCM) of Tunisia. The purity of both compounds was ≥99% and suitable for pharmaceutical applications. Methanol of analytical grade was purchased from Sigma Aldrich and used as such. Ultrapure Millipore water used in the study was generated in the laboratory. Supersaturated aqueous suspensions of K_2SO_4, KCl, and NaBr and pure, dry P_2O_5 were used in desiccators to control the relative humidity at levels of 98, 84, 57.6, and 0 % RH, respectively.

2.2 Preparation of the amorphous solid dispersions

Pure samples of atorvastatin and solid dispersions with different weight fractions of PVP K40 (0.05, 0.10, 0.25, 0.50, 0.60, and 0.75) were prepared by three different amorphization techniques: ball milling, spray drying and freeze drying.

2.2.1 Ball milling

Samples were milled for a total of 4 hours in shock mode and a rotation couple of 700/-700 rpm using a Fritsch Pulverisette P7 Premium Line Planetary Ball Mill using zirconium oxide containers and zirconium oxide balls with a diameter of 10 mm. In order to limit the heating of the sample during the grinding process, grinding periods of 20 min were interchanged with a 5 min pause until the sample had been effectively milled for 4 h. The total time interval had been determined through preliminary milling experiments and X-ray diffraction indicating that complete amorphization had been reached after 4h of effective milling (i.e., no diffraction peaks could be observed anymore in the X-ray diffraction patterns). A fixed amount of 1 g of total sample was used in each milling experiment. After milling, the samples were stored in an airtight silica gel container for later study.

2.2.2 Spray drying

For each of the ATC-PVP K40 mixtures with the aforementioned weight fractions, one gram was dissolved in 100 mL of methanol at room temperature and clear solutions were obtained. Spray drying of these solutions was carried out using a Büchi Mini Spray Dryer B-290 with a 0.7 mm nozzle under the following conditions: an inlet temperature of 120 °C, an outlet temperature of 64 °C, a feed rate of 1 $mL \cdot min^{-1}$ and a nitrogen flow at 40 $mL \cdot min^{-1}$. The obtained particles were stored in a desiccator until further use.

2.2.3 Freeze drying

Mixtures with the same weight fractions based on atorvastatin and polymer (PVP K40) were dissolved in a 10-90 v/v% water-methanol mixture at room temperature with a concentration of 1g per 100 ml. The rotary evaporator was used to remove the methanol at 35°C after complete dissolution, because the freeze dryer was not adapted to be used with organic solvents. The obtained liquid was then frozen using liquid nitrogen. Finally, it was transferred to a Christ Alpha 2-4 Freeze Dryer for freeze drying. The liquid after removal of the methanol was white, indicating that ATC did not remain in solution, however, no precipitate was observed in the flasks, so that the solid must have consisted of small particles in the order of micrometers dispersed in the polymer water phase. Although this will have an effect on the final freeze-dried phase, the preparation method will be referred to in the text as freeze-drying.

2.3 Characterization methods

2.3.1 Differential Scanning Calorimetry

Differential Scanning Calorimetry (DSC) was carried out with the DSC 214 Polyma Netzsch using aluminum pans with about 4 mg of samples, under a dynamic nitrogen atmosphere. For all experiments, the covers of the aluminum pans were pierced to allow residual water to evaporate during heating while purging with dry nitrogen gas. The DSC instrument is equipped with a 20-position sample changer and an intracooler that allows measurements down to -70 °C. Temperature scans were carried out from 20 to 200 °C with a heating rate of 5 $K\ min^{-1}$.

2.3.2 X-ray powder diffraction

X-ray diffraction (XRD) experiments were carried out at room temperature using a D8 Discover diffractometer (Bruker Analytic X-ray Systems, Germany) with the Bragg-Brentano geometry.

The instrument is equipped with a copper anticathode [40 kV, 40 mA, Kα radiation (λ = 1.5406 Å)] and a lynxeye linear detector. The samples were placed under a thin glass cover slip. X-ray diffraction analyses were performed with a step size of 0.04° 2θ, with 0.5 s/step from 3 to 30° 2θ. The φ rotation of the sample specimen holder minimizes the effects of texture and preferential orientation.

2.3.3 Second harmonic generation

Because atorvastatin is a chiral molecule, and the crystal of its calcium salt hydrate possesses an SHG signal, the SHG technique could be used to rapidly detect the onset of its crystallization (Galland et al. 2009). An Nd:YAG Q-switched laser (Quantel) operating at 1.064 µm was used to deliver 360 mJ pulses of 5 ns duration with a repetition rate of 10 Hz. An energy adjustment device made up of two polarizers (P) and a halfwave plate (λ/2 = 532 nm) allowed the incident energy to be varied from 0 to ca. 200 mJ per pulse. An RG1000 filter was used after the energy adjustment device to remove light from the laser flash lamps. Following Kurtz and Perry's SHG powder method (S. K. Kurtz et T. T. Perry 1968), the signal intensities were compared to that of the reference compound quartz (45 µm average size).

2.3.4 Physical stability studies

The amorphous ATC-based dispersions were stored in moisture-controlled desiccators for one year to study their physical stability and their ability to absorb water. The following relative humidities (RH) were used at 20°C: 0 %, 57.6 %, 84%, and 98%. 100 mg of each sample was subjected to the humidity in the desiccators in 20 ml scintillation vials.

3 Results

3.1 Physical characterization of amorphous atorvastatin calcium

3.1.1 Grinding time necessary to obtain amorphous atorvastatin calcium

In Fig. 1, the X-ray diffraction patterns of ATC as a function of different milling (700 rpm) intervals are shown. The diffraction pattern of the unground drug exhibits the characteristic diffraction peaks of the crystalline trihydrate of ATC. Up to about two hours of milling, ATC retains some crystallinity even if the diffraction intensity decreases (Fig. 1). After four hours of grinding, no visible trace of crystallinity is left in the diffraction pattern (Fig. 1) and only the amorphous halo can be observed, which is characteristic of materials without long-range order. The absence of any observable crystallinity is confirmed by DSC (see Fig. 2) and by SHG (Table S1 in the supplementary materials). Thus, throughout this article, samples amorphized by milling have been ground for at least 4 hours at 700 rpm. For reference, in Fig. S1 in the supplementary materials, the powder X-ray diffraction (PXRD) and DSC data for crystalline and amorphous atorvastatin calcium (ATC) are provided.

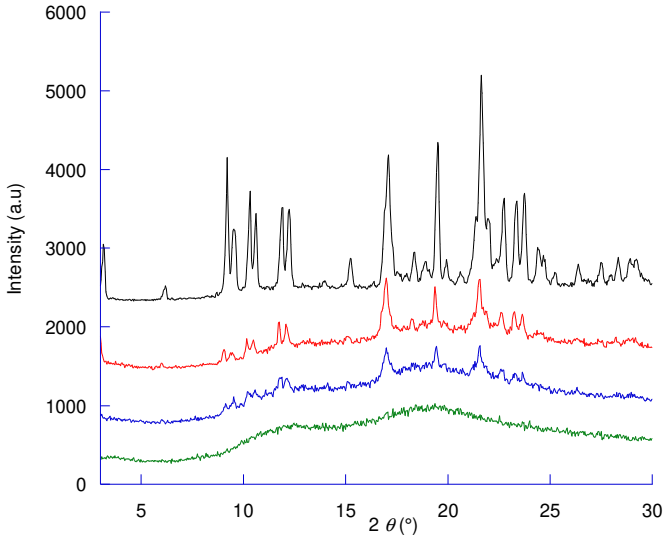

Fig. 1. X-ray diffraction patterns of ATC subjected to milling at 700 rpm in a planetary mill for different time intervals: no milling (black), 1 hour (red), 2 hours (blue) and 4 hours (green).

3.1.2 Comparison between the ATC amorphous states obtained by different methods

Figure 2a presents the PXRD patterns of crystalline atorvastatin recorded at room temperature after different treatments (from bottom to top): melting, milling, spray and freeze drying. None of the diffraction patterns contain clear Bragg peaks, indicating that all processes produced amorphous atorvastatin within the detection limitations of X-ray diffraction (Fig 2a). These findings were confirmed by DSC (Fig. 2b) and SHG (Table S1 in the supplementary materials). In the case of the freeze-dried sample, it does indicate that an amorphous phase is obtained even though a dispersion was freeze-dried instead of a clear solution. Overall, the diffraction patterns are similar, showing two broad features in the scattering halo. Nonetheless, at around 3° 2θ, a small peak can be observed in the patterns of the samples obtained by fusion (black), spray drying (green), and freeze drying (blue). This is the signature of a liquid crystal-like laminar structure, linked to the mesophase of dehydrated atorvastatin calcium previously mentioned in the literature; thus, in these three samples some long-range order remains present (Christensen et al. 2013). Any other structural differences between the amorphous states are too small to be detected by classical X-ray diffraction.

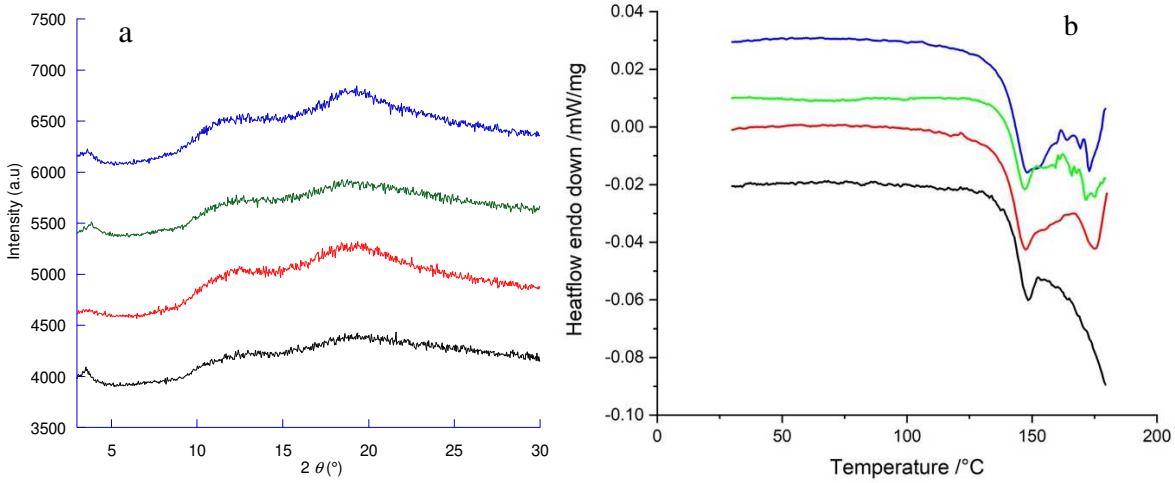

Fig. 2. (a) Powder X-ray diffraction patterns and **(b)** differential scanning calorimetry curves of amorphous atorvastatin calcium obtained by fusion (black), milling (red), spray drying (green), and freeze drying (blue). The DSC curves have been recorded after an initial heating run up to 120°C to remove residual water. The increase of the baseline after the glass transition is probably due to decomposition. For pure crystalline atorvastatin calcium decomposition tends to start above 170° C (Tizaoui et al. 2020).

The DSC thermograms (Fig. 2b) each exhibit a characteristic heat capacity drop indicative of a single glass transition, demonstrating that the samples are in a vitreous state at room temperature. No exothermic peaks are observed indicating that no crystallization occurred in the heating runs at a heating rate of 5 K·min^{-1}. The glass transition temperatures of the four amorphous ATC samples possibly depend slightly on the amorphization method, as the following values (midpoint) were found: fusion 143 ±1 °C, milling 142 ±1 °C, spray drying 143 ±1 °C, and freeze drying 143 ±1 °C.

3.2 Solid dispersions of atorvastatin calcium and PVP

3.2.1 Comparison between the different amorphization methods

Milling, spray drying, or freeze drying has been applied to three sets of mixtures containing ATC and PVP with mass percentages of 0%, 5%, 10%, 25%, 50%, 60%, 75%, and 100% PVP. Melting was not used for amorphization due to concerns about the decomposition of ATC at high temperatures (Shete et al. 2010). Diffraction patterns and thermograms for the different mixtures have been compiled in the Figs. 3 to 5. The midpoint temperatures of the observed glass transitions can be found in Table 1.

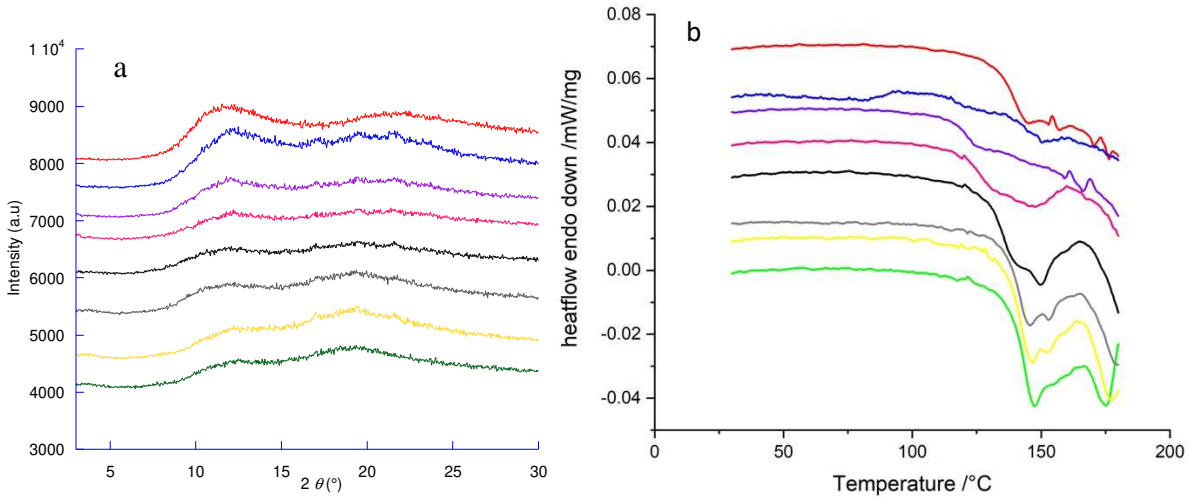

Fig. 3. (a) PXRD patterns and **(b)** DSC thermograms (5 K·min^{-1}) of amorphous atorvastatin calcium and PVP K40 dispersions prepared by four hours of milling with the following concentrations in PVP mass % from bottom to top: 0 (green), 5 (yellow), 10 (grey), 25 (black), 50 (pink), 60 (violet), 75 (blue) and 100 (red).

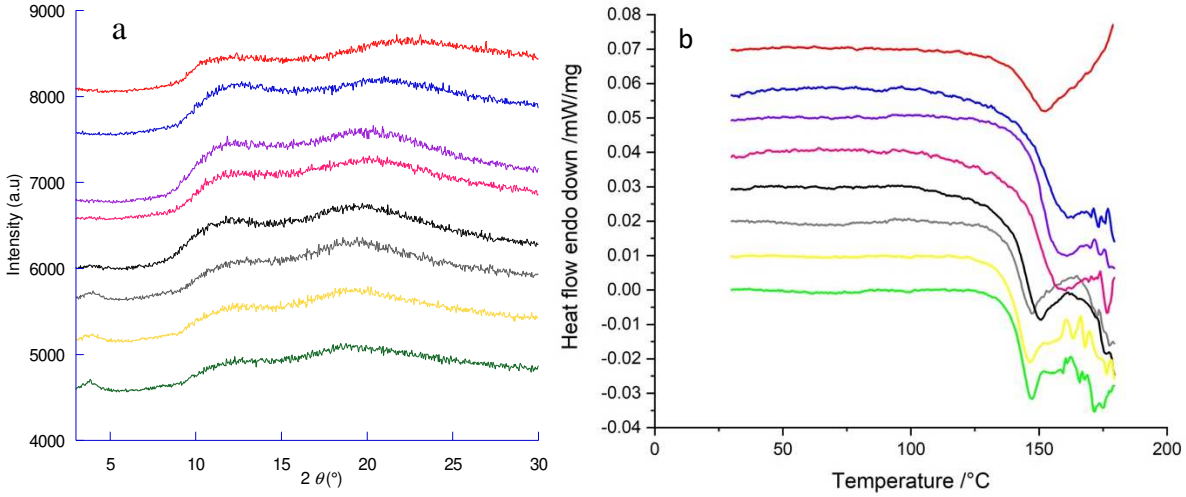

Fig. 4. (a) PXRD patterns and **(b)** DSC thermograms (5 K·min^{-1}) of amorphous atorvastatin calcium and PVP K40 dispersions prepared by spray drying with the following concentrations in PVP mass % from bottom to top: 0 (green), 5 (yellow), 10 (grey), 25 (black), 50 (pink), 60 (violet), 75 (blue) and 100 (red).

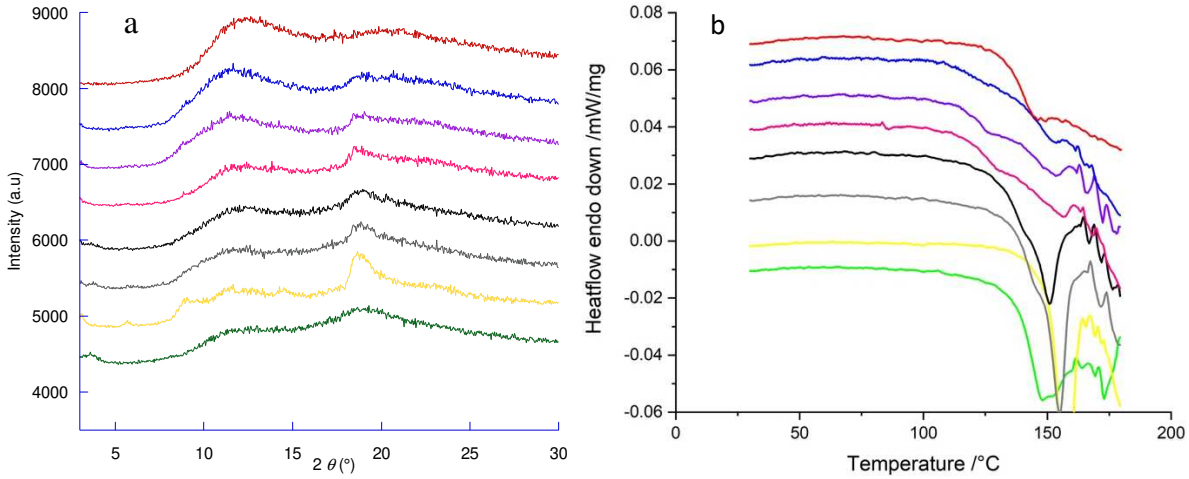

Fig. 5. (a) PXRD patterns and **(b)** DSC thermograms (5 K·min^{-1}) of the amorphous atorvastatin calcium and PVP K40 dispersions prepared by freeze drying with the following concentrations in PVP mass % from bottom to top: 0 (green), 5 (yellow), 10 (grey), 25 (black), 50 (pink), 60 (violet), 75 (blue) and 100 (red).

All three methods, milling, spray drying, and freeze drying, produced mainly amorphous material (Figs. 3 to 5). In the case of freeze drying, however, some extra features can be observed in the PXRD patterns, which are most pronounced for the 5 wt% PVP at around 18° 2θ, which is characteristic of the mesophase of ATC (Tizaoui et al. 2020; Christensen et al. 2013). A similar observation can be made in the DSC curves of 5, 10 and 25 wt%, which have an additional endothermic peak located at the melting point of the mesophase (Tizaoui et al. 2020; Christensen et al. 2013). The appearance of the mesophase of ATC may be due to the formation of liquid dispersions during the preparation of the freeze-drying experiments instead of clear solutions. Surprisingly, ATC with 0% PVP appears to be fully amorphous according to

the thermogram and no additional features are observed in the diffraction pattern, except for a shallow peak at 3° 2θ indicative of some lamellar structuration in the amorphous phase. It seems therefore that the presence of PVP causes a certain level of structuration in the ATC during freeze drying preparation resulting in the formation of a mesophase-like structure. Moreover, in the spray-dried samples, the lamellar structure that was observed for pure amorphous ATC remains present up to 10% and possibly 25% of PVP as the small diffraction peak at 3° 2θ indicates.

Analysis by second harmonic generation microscopy (See Table S1) shows that none of the dispersions prepared by the three methods exhibit an SHG signal, whereas the signal of crystalline atorvastatin trihydrate has an intensity of 652 counts. The SHG method is very sensitive to non-centrosymmetric (NC) materials reaching in favorable cases a detection threshold at ppm level for NC crystals in an amorphous matrix (Clevers et al. 2013). It confirms that any structuration seen in the X-ray diffraction patterns must be the result of a mesophase and not of small ATC crystallites dispersed in the amorphous solid, because they would have generated an SHG signal.

3.2.2 Glass transitions

The glass transition temperatures from the milled and the freeze dried samples are extremely similar, whereas those of the spray dried samples deviate considerably (Table 1). Although it is known that the glass transition temperature varies depending on the measurement method and on the heating rate, the present measurements are all carried out with a heating rate of 5 $K \cdot min^{-1}$.

The dispersions obtained with spray drying exhibit the highest glass transition temperatures (T_g) (see Table 1); there is a slow upward drift in these temperatures over the entire concentration range after an initial dip at 5 % PVP that still coincides with the other two amorphisation methods. The implications are not clear. An increase in the T_g implies a stabilization of the glassy phase and the single drop in the baseline of the DSC curve implies a complete mixture, or at least that any other phase present is too small in size to leave a significant thermal signature. It can be seen however, that pure PVP is affected too by spray drying, so the observed effect may be related to the interactions between PVP and methanol under spray drying conditions.

For milled and freeze-dried samples a decrease in the T_g can be observed as a function of the polymer concentration. The single drop in each DSC curve indicates the formation of a molecular dispersion of the two components, i.e. a single mixed phase. However, for milling at 75% PVP and for freeze drying at 60 and 75 % PVP, the single T_g disappears and is possibly replaced by two glass transitions of which the midpoints are hard to determine due to lack of sufficiently clearly defined baselines. In any case, it is clear that optimal mixing at these concentrations is not reached with either milling or freeze-drying.

With freeze drying, the T_g's in the mixtures 5, 10 and 25 % PVP are convoluted with the melting peak of the mesophase, which is known to occur at 150°C (see Figure 5b), so it may be concluded that mixing is not ideal, which is probably caused by the crashing out that happened at the preparation stage of the freeze-drying process. However, there may also be a possibility that the mesophase is incorporated in the mixture, because the mesophase is mostly amorphous (Tizaoui et al. 2020; Christensen et al. 2013)) and the T_g's of the samples closely follow the values of the milled samples.

Table 1. Glass transition temperatures (T_g) measured by DSC of the atorvastatin calcium/PVP mixtures obtained by milling (M), spray drying (SD), and freeze drying (F)[a]

PVP content (wt%)	T_g - M (°C)	T_g - SD (°C)	T_g - F (°C)
0	142(1)	143(1)	143(1)
5	140(1)	141(1)	-[b]
10	139(1)	143(1)	139(1)
25	136(1)	145(1)	135(1)
50	125(1)	149(1)	124(1)
60	121(1)	151(1)	122(1)[c]
75	-[c]	151(3)	-[c]
100	138(1)	146(1)	138(1)

[a] Standard deviation of the data has been given in parentheses

[b] T_g convoluted with a melting peak; not enough baseline to determine value

[c] Samples do not appear monodisperse; hard to determine T_g values

3.2.3 Comparison between measured and calculated X-ray diffraction patterns

In the Supplementary Materials the diffraction patterns of the different mixtures (Figs. S2, S3, and S4) are compared and discussed. It should be remarked here though that in the case of freeze drying (Fig. S4), long-range order can be observed in these samples by the presence of low-intensity diffraction peaks at around 18° 2θ and possibly also at 11°. The long-range order is corroborated by the DSC results, in which for the higher ATC concentrations the mesophase peak can be observed (Tizaoui et al. 2020; Christensen et al. 2013). Although, it is likely that in the case of freeze drying the use of water in the solvent mixture, in which PVP is soluble, but ATC is not, has simply not induced complete mixing of the two components on a molecular level, a single glass transition temperature up to 50 % PVP appears to indicate that mixing and structuring at a mesoscale level are not mutually exclusive phenomena and have been promoted by the freeze drying process. This may have happened already at the preparation stage when the methanol was removed from the solution and a liquid dispersion was formed. It has been clearly demonstrated in previous studies that after the removal of the crystal water from the ATC trihydrate a mesophase remains (Tizaoui et al. 2020; Christensen et al. 2013). Interestingly, the pure ATC sample appears to be more amorphous than those containing polymer, indicating that PVP somehow promotes the formation of the mesophase in freeze drying.

3.2.4 The glass transition temperature as a function of the composition

In Fig. 6, the evolution of the glass transition temperature of the different solid dispersions is shown as a function of the ATC weight fraction.

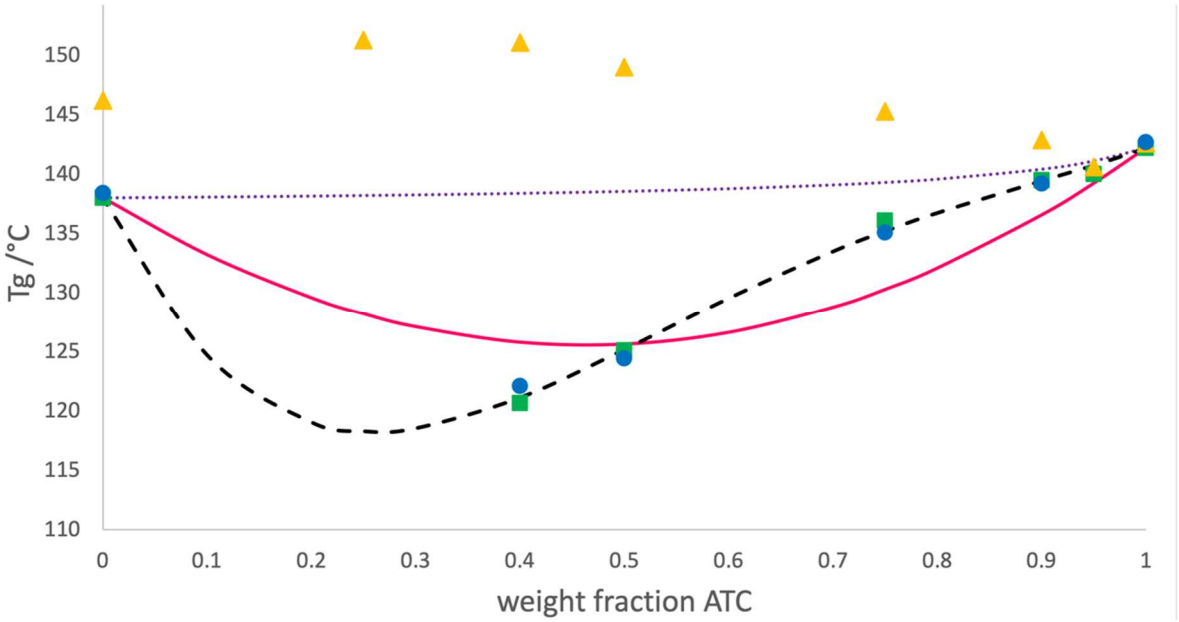

Fig. 6. Glass transition temperatures of the ATC-PVP mixtures as a function of the PVP weight fraction obtained by milling (green squares), by freeze drying (blue circles), and by spray drying (yellow triangles) and determined by DSC. The dotted purple line is the Gordon-Taylor relationship (for illustration only), while the solid red and dashed black lines are fits of the milling data with the Kwei and Brostow equations, respectively. These fits are a guide to the eye as the number of weight fractions is too limited for reliable 3-parameter fits.

A common description of the glass transition temperature as a function of composition is the Gordon-Taylor expression (Gordon et al. 2014):

$$T_{g,mix} = \frac{w_1 \mathrm{Tg(PVP)} + K w_2 \mathrm{Tg(ATC)}}{w_1 + K w_2} \quad (1)$$

Where the constant K, which in the original paper represents the change in the difference in specific volume between the glassy and the liquid phase with temperature, can be approximated by:

$$K = \frac{\rho_1 \mathrm{Tg(ATR)}}{\rho_2 \mathrm{Tg(PVP)}} \quad (2)$$

In these expressions, T_g(ATR) and T_g(PVP) represent the glass transition temperatures of pure atorvastatin and pure PVP, respectively. w_1 corresponds to the mass fraction of PVP in the mixture and w_2 to that of ATC.

It is clear from Fig. 6 that spray drying and the other two amorphization methods produce completely different results in terms of the glass transition temperatures and of their evolution of T_g versus composition. Spray drying appears to slightly raise the glass transition temperature of the mixtures, but considering the descent in glass transition temperatures for the other two methods, it is not clear how an attractive interaction between the API and the polymer may exist that would only be triggered in spray-dried mixtures. Nonetheless, both polymer and API are

amorphous and there appears to be one single phase with a single glass transition, but how the two components are mixed together is not clear at this stage. Methanol, which is used as the spraying solvent and which is a reasonable good solvent for both ATC and PVP, may play a role. It can also be observed that PVP alone exhibits a significant increase in its glass transition temperature when spray dried in methanol.

The glass transition temperatures of the milled samples and of the freeze-dried samples appear to provide a picture of somewhat homogeneous mixtures up to about 60% PVP with a clear minimum in the glass transition temperature as a function of the composition. The T_g behavior cannot be fitted with the Gordon-Taylor equation nor with the Kwei equation (Kwei 1984; Kalogeras 2010) as the red line in Fig. 6 demonstrates (K_{kwei} = 1 and q = −58.0). A better fit can be obtained by an expression proposed by Brostow et al. (Brostow et al. 2008) leading to the fitting parameters a_0 = −59.7, a_1 = −79.1, and a_2 = -46.1 (Kalogeras 2010) (See the supplementary information for the equation S1). Problematic for the latest fit is that there are not enough data points (weight fractions) to warrant an equation with three variables, even if both milled and freeze-dried T_g data are fitted together. So, the dashed line is principally a guide to the eye.

Considering the clear negative deviation of the glass transition in both milling and freeze-drying samples, the interactions between ATC and PVP do not appear to be favorable for mixing. This is however contradictory to the results obtained by spray drying, which need more study to understand the cause behind the increase in T_g with a maximum around the weight fractions of 60 and 75 %, although the combination of methanol and PVP may create conditions in which the glass transition increases.

3.3 Stability of amorphous solid dispersions of ATC and PVP as a function of the relative humidity

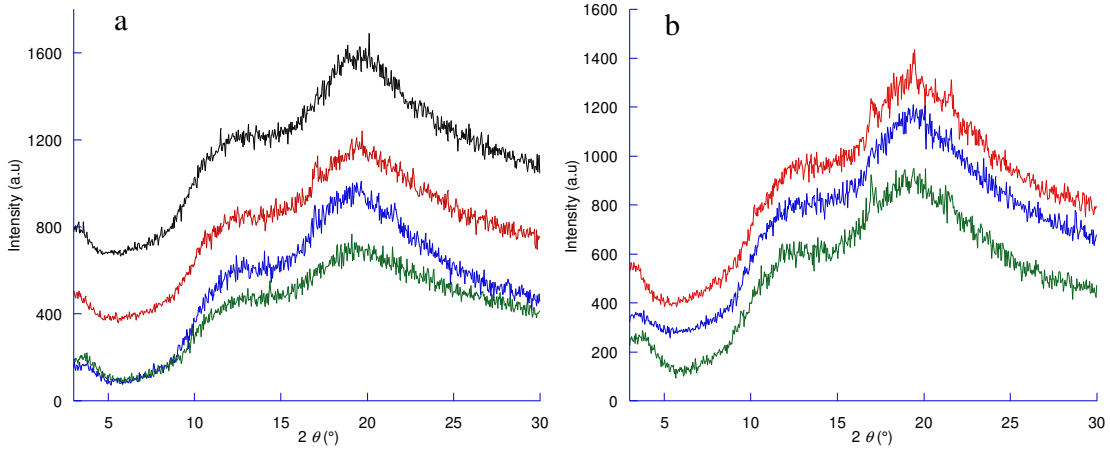

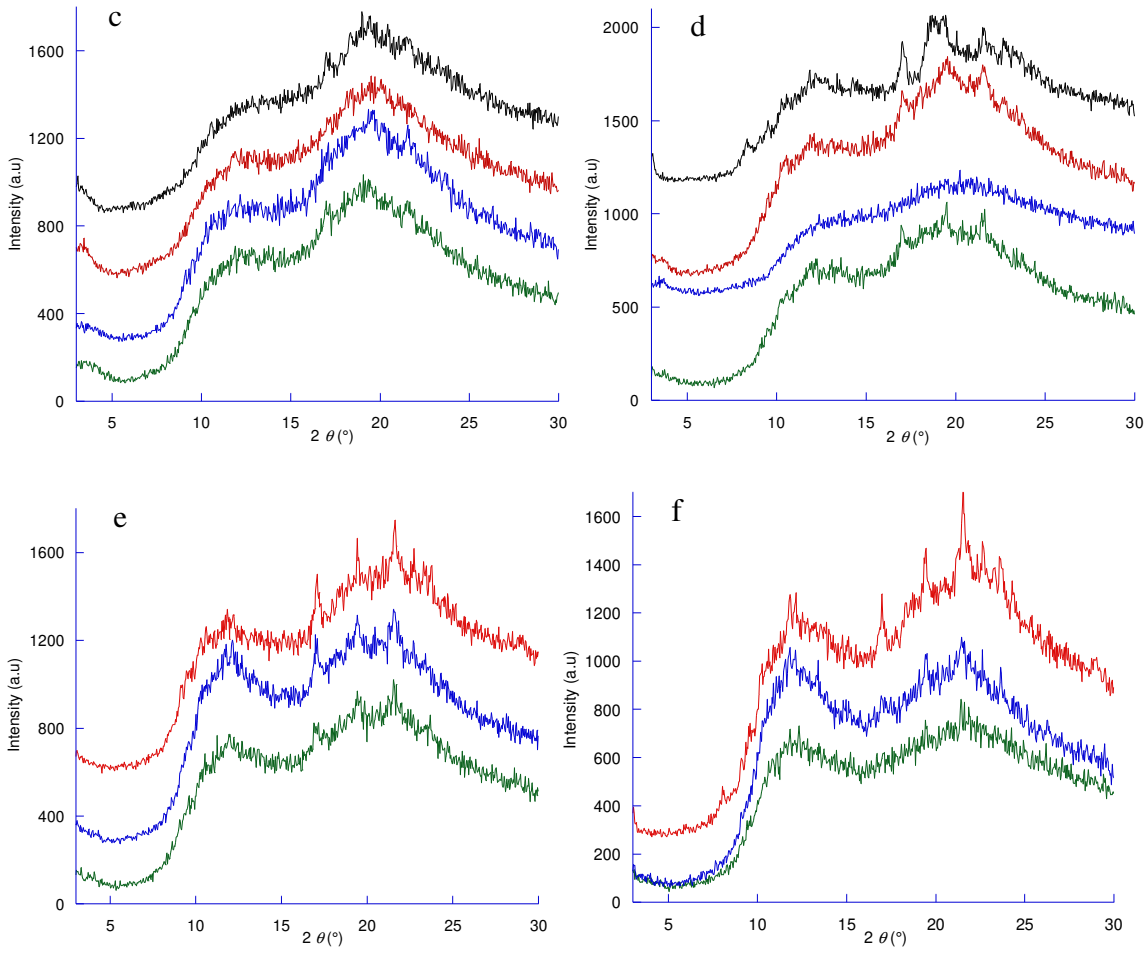

Fig. 7. PXRD patterns of ATC-PVP amorphous dispersions prepared by milling with **(a)** 0% PVP, **(b)** 5% PVP, **(c)** 10% PVP, **(d)** 25% PVP, **(e)** 50% PVP, and **(f)** 75% PVP after one year of storage at moisture levels of 0 % RH (green), 57 % RH (blue), 84 % RH (red), and 98 % RH (black) at room temperature

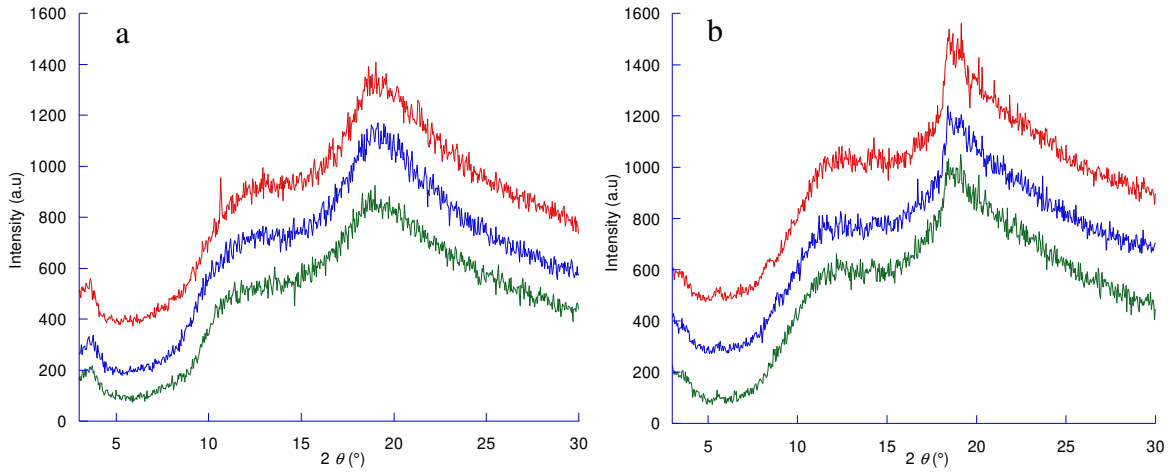

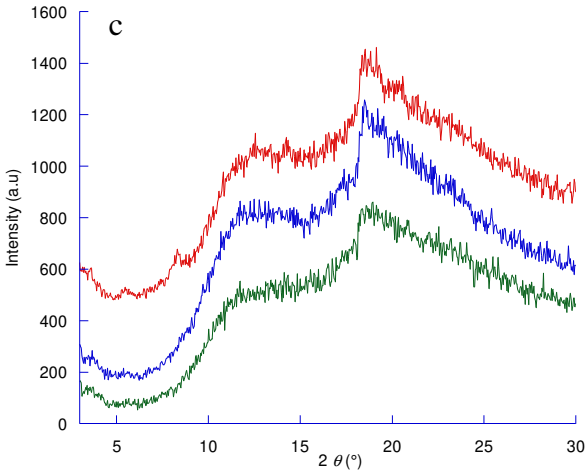

Fig. 8. PXRD patterns of ATC-PVP amorphous dispersions prepared by freeze drying with **(a)** 0% PVP, **(b)** 10% PVP, and **(c)** 25% PVP after one year of storage at moisture levels of 0 % RH (green), 57 % RH (blue), and 84 % RH (red), at room temperature

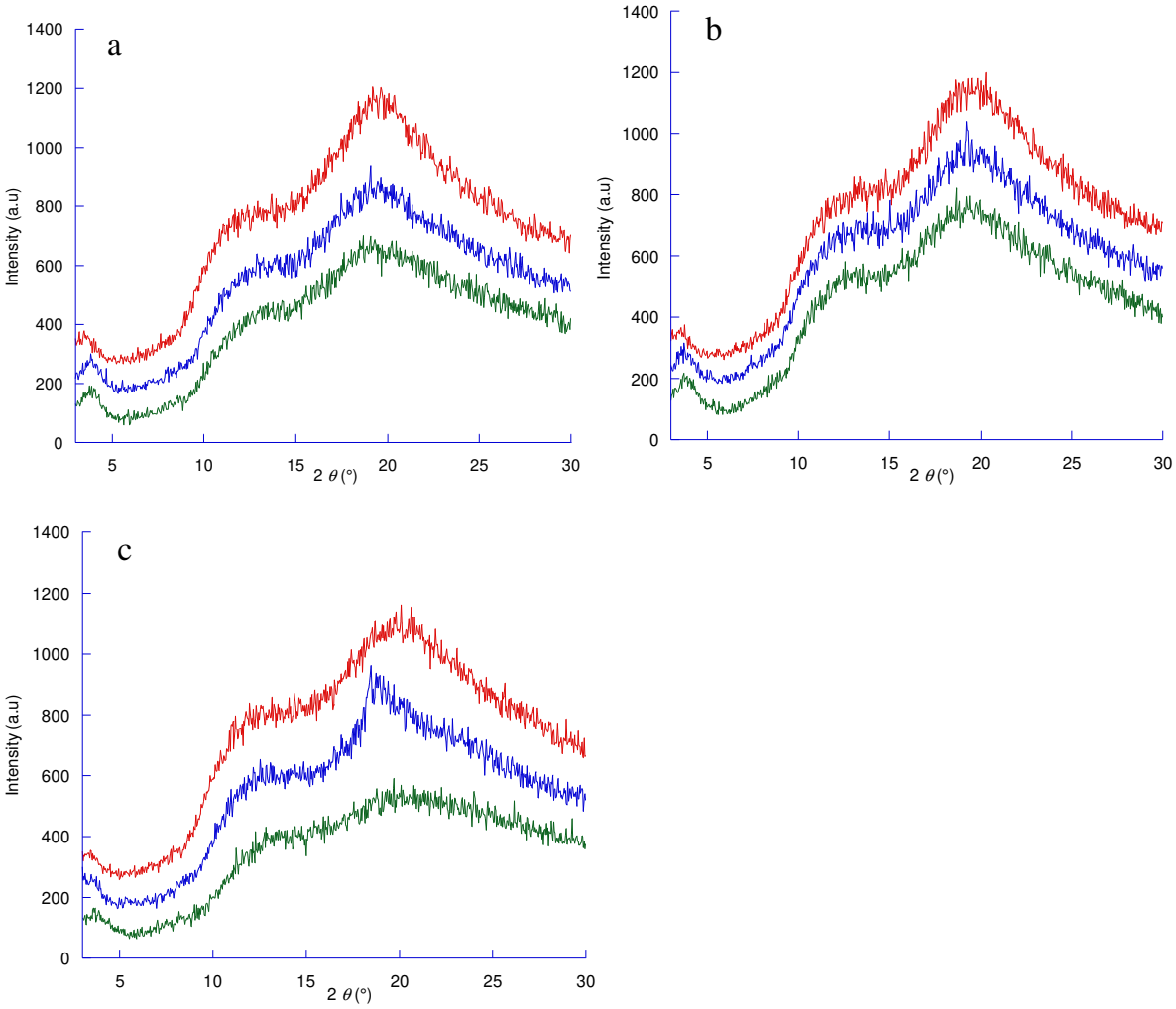

Fig. 9. PXRD patterns of ATC-PVP amorphous dispersions prepared by spray drying with **(a)** 0% PVP, **(b)** 10% PVP, and **(c)** 25% PVP after one year of storage at moisture levels of 0 % RH (green), 57 % RH (blue), and 84 % RH (red), at room temperature

All amorphous solid dispersions of ATC-PVP take up water when subjected to increased humidity levels and the higher the humidity, the higher the water take-up (Figs. S5, S6, and S7); however, the increase in water content is mostly due to adsorption as, in most cases, it does not lead to crystallization of the ATC trihydrate.

Milled ATC, stored at room temperature without polymer, demonstrates little tendency to crystallize even under high humidity levels. In fact, the mixtures with a high content in PVP exhibit a higher tendency to crystallize into the ATC trihydrate, even at low relative humidities. It suggests that PVP may retain water or promote the capture of water that can subsequently be used for recrystallisation of the ATC trihydrate (Fig. 7 and Fig. S8 in the supplementary materials). Despite, the observation of typical trihydrate peaks, the level of crystallinity remains extremely low, in the order of a few percent of the sample, even after one year. For dispersions prepared by milling, an SHG signal appears after a year with increasing moisture content at PVP percentages above 10 % (Table S1 and Fig. S12 in the supplementary materials).

In the samples obtained by freeze drying, little recrystallisation occurs over the timeframe of a year, however, the mesophase, whose existence was already remarked just after amorphisation remains, in particular for the samples containing polymer (Fig. 8). ATC without polymer and amorphized by freeze drying appears to resist recrystallisation whether in a dry environment or subjected to high humidity (Figs. 8 and S10) and the lamellar structure, indicated by the small peak at 3° 2θ, does not appear to have any destabilizing effect. For a single sample prepared by freeze drying with 10% PVP and subjected to 57% RH after one year, an SHG signal is observed, indicating that NC crystallites have appeared in the sample, even if this was not obvious from the XRPD results. No other freeze-dried samples exhibit recrystallisation however (Table S1 and Fig. S13).

Samples obtained by spray drying demonstrate little change over the timeframe of a year (Fig. 9). One sample with 25% PVP and a relative humidity of 57% exhibits a single peak-like feature at around 19° 2θ, which probably indicates an onset of crystallization, but this is not certain as no other peaks are present. It may again demonstrate that high polymer content causes the samples to be more prone to changes over time. The SHG signal of the dispersions prepared by spray drying remains zero even with a high moisture content (Table S1 and Figs. S9 and S14).

3.4 The influence of the polymer concentration on the stability of the amorphous dispersions

In Figs. S15 and S19, it can be seen that the milled samples crystallize to a larger extent when more PVP is present in the mixtures. In addition, an increase in humidity from 57 to 84 % RH also appears to promote crystallization. Samples without PVP or containing very little PVP are the most persistent over time and under high humidity levels.

The dispersion with 75% PVP formed a sticky paste already after 10 days, while the other dispersions remained powdery, demonstrating the instability of solid dispersions containing high concentrations of PVP K40. PVP generally suffers from such instability, especially under conditions of high relative humidity (Caron et al. 2013).

The presence of PVP in freeze drying clearly promotes the formation of the mesophase and consequently a certain level of structuration is present in the samples afterwards. This appears to lead to some crystallization of the ATC after a year as SHG signals appear in the 10% PVP samples, whereas samples without PVP remain amorphous (Figs. S16 and S20).
In the case of spray drying, basically no crystallization is observed for any of the samples and so neither the PVP concentration nor the relative humidity seem to affect the amorphous state (Figs. S17 and S21), even if the samples with no or little PVP content do exhibit a sort of long-range lamellar structure as indicated by the small peak at 3° 2θ in the diffraction patterns.
Thus, overall, the data demonstrates a destabilizing effect of PVP on the amorphous state of ATC, because the milled samples with PVP crystallize more readily, and to a lesser extent the freeze-dried samples too. In the spray-dried samples, the increase in the T_g may in part explain why very little crystallization is observed. Finally, amorphous samples that do not contain PVP, either milled, spray-dried, or freeze-dried do not crystallize at all (Figs. S19-S21).

3.5 The influence of the amorphisation method on the stability of the amorphous dispersion

Comparing the different methods, it is clear that, even if water take-up did not particularly depend on a method (Fig. S11), milled samples are more prone to recrystallization, in particular under high relative humidities, whereas amorphization methods with solvent increase the chance of forming a mesophase-like structure in the presence of polymer (Fig. S22). Spray-dried samples for which methanol was used exhibit the least recrystallisation tendency (Fig. S22), which is confirmed by second harmonic generation spectroscopy (Fig. S18).

4 Discussion

Ball milling appears to produce a single phase, well-dispersed amorphous drug as shown by the single T_g values up to 60% PVP. However, the negative deviation in the glass transitions as a function of polymer content demonstrate a weak, unfavorable interaction between the API and the polymer. In milling, material departs from a solid crystalline state and amorphization is the result of the creation of disorder in the initially ordered crystalline matrix and therefore nanocrystals or semi-structured nanodomains, not observable by X-ray diffraction, may still remain in the sample (Bates, S. et al. 2006). The combination of remaining crystalline nuclei after milling and the weak unfavorable ATC-polymer interaction may lead to the observed recrystallisation that, although slowly, occurs in most of the milled samples. In this respect it is striking to see that the samples not containing PVP show least tendency to recrystallize, and the polymer therefore clearly exhibits a destabilizing effect. The fact that PVP and ATC are both hygroscopic may trap a certain amount of water in the milled samples and the plasticizing effect of water may explain part of the decrease observed in the glass transition temperatures (Rumondor et al. 2009).

Freeze-drying exhibits similar results in terms glass transition temperatures; however, the mesophase is clearly present in almost all samples. Less recrystallisation may be explained by the absence of any prior crystalline nuclei, due to the dissolution stage in the amorphization process. There is also an indication that the system in the case of freeze-drying and in the case

of milling has a problem in deciding itself about its state above approximately 60% PVP, where the well-defined T_g seems to disappear and possibly gets replaced by two T_g's, but their respective values are hard to determine due to a lack of a clear baseline. It is well known in the literature that solvents and drying of drug-polymer dispersions can have significant effects on their demixing (Dohrn, S. et al. 2021 ; Dohrn, S. et al 2020 ; Boel, E et al. 2021). These effects may also play a role in the freeze-drying experiments.

The presence of methanol and the differences in solubility of the polymer and ATC during preparation of the spray-dried samples may have led to a rather specific phase being produced as the increase in T_g indicate, although more study is needed to better understand the behavior of PVP under these conditions and of these mixtures.

5 Conclusions

In this paper, the influence of the amorphization pathways, of polymer content, and of the moisture levels during storage on the physical state of atorvastatin-polyvinylpyrrolidone solid dispersions has been studied. Three amorphization methods were explored: high-energy milling, freeze drying, and spray drying.

Milling leads to samples that tend to recrystallize, albeit slowly. The presence of PVP accelerates recrystallisation, whereas the influence of the level of relative humidity is less clear. A negative deviation of the glass transition temperature as a function of the PVP composition clearly indicates that the interaction between ATC and PVP is not favorable within mixtures obtained by milling.

Freeze drying leads to structuration in the samples in the form of a mesophase when PVP is present, while the decrease in the glass transition temperature indicates that mixing between polymer and API is similar to that of the milled samples. The mesophase may be due to the formation of a liquid dispersion in the preparation stage of the spray drying experiment. Samples without PVP do not tend to crystallize for over a year, whereas PVP containing samples exhibit some level of structuration and crystallization. The level of relative humidity appears to be of lesser importance for crystallization, as long as some water is present for the formation of the ATC trihydrate.

Spray drying leads to samples with increased glass transition temperatures, which implies a certain stabilization of the mixtures and for pure PVP. This is also borne out by the high-humidity storage experiments, because neither samples with nor without PVP exhibit much tendency to crystallize over the time of a year. Hence, the amorphization method and most likely the solvent, methanol, in combination with PVP affects the stability of mixtures considerably and the interactions between the polymer and the API as well as the interactions with the solvent used during the amorphization seem to play important roles.

There was no clear difference in the effect of the amorphization method on recrystallization of pure ATC, as it did not occur for any of these samples.

In the case of atorvastatin calcium, its amorphous state and the high glass transition temperature clearly give the API sufficient stabilization against recrystallisation even in the presence of water vapor. PVP destabilizes the amorphous state of atorvastatin calcium under certain conditions, either by structuring the samples to some extent or by functioning as a source for water molecules. From the current experiments, spray drying of atorvastatin calcium (in the

absence of PVP) leads to the most persistent amorphous samples that resist crystallization for over a year even in the presence of water vapor.

Acknowledgements

The authors thank Stéphane Leleu of the IUT of the University of Rouen for his help with the freeze-drying experiments. C Tizaoui thanks the Tunisian Ministry for Higher Education and Scientific Research for a scholarship of 6 months.

Declarations of interest: none

References

Adibkia, Khosro, Mohammad Barzegar-Jalali, Hosein Maheri-Esfanjani, Saeed Ghanbarzadeh, Javad Shokri, Araz Sabzevari, et Yousef Javadzadeh. 2013. « Physicochemical Characterization of Naproxen Solid Dispersions Prepared via Spray Drying Technology ». *Powder Technology* 246 (septembre): 448-55. https://doi.org/10.1016/j.powtec.2013.05.044.

Arunkumar, N, M Deecaraman, C Rani, K P Mohanraj, et K Venkates Kumar. « Preparation and solid state characterization of atorvastatin nanosuspensions for enhanced solubility and dissolution », *Int.J. PharmTech Res*.2009,1(4).

Bates, S.; Zografi, G.; Engers, D.; Morris, K.; Crowley, K.; Newman, A., Analysis of amorphous and nanocrystalline solids from their X-ray diffraction patterns. *Pharm. Res.* **2006,** *23* (10), 2333-2349.

Bhumika Sharma, . Vikrant Saini, et . Arvind Sharma. 2012. « Preparation, Characterization and In-Vitro Evaluation of Atorvastatin Calcium Solid Dispersions with Various Hydrophilic Polymers and Its FDT Formulation. » *Journal of Current Pharma Research* 2 (4): 620-30. https://doi.org/10.33786/JCPR.2012.v02i04.003.

Bobe, K R, C R Subrahmanya, Sarasija Suresh, D T Gaikwad, M D Patil, T S Khade, B B Gavitre, V S Kulkarni, et U T Gaikwad. 2011. « Formulation and evaluation of solid dispersion of atorvatstatin with various carriers » *Pharmacie Globale© (IJCP)*, Vol. 02, Issue 01.

Boel, E.; Giacomini, F.; Van den Mooter, G., Solvent influence on manufacturability, phase behavior and morphology of amorphous solid dispersions prepared via bead coating. *Eur. J. Pharm. Biopharm.* **2021,** *167*, 175-188.

Briggs, C. A., Jennings, R. A., Wade, R., Harasawa, K., Ichikawa, S., Minohara, K., and Nakagawa, S. **_1999_**. "Crystalline _R-_R*,R*__-2-_4 Dfluorophenyl_-_ ,_-dihydroxy-5-_1-methylethy l_-3- phenyl-4-__phenylamino_carbonyl_-1H-pyrrole-1-heptanoic acid hemi calcium salt _atorvastatin_," Patent Assignee Warner-Lambert Co., Application No. 08/945,812, US005,969,156A, 19 October 1999.

Brostow, Witold, Rachel Chiu, Ioannis M. Kalogeras, et Aglaia Vassilikou-Dova. 2008. « Prediction of Glass Transition Temperatures: Binary Blends and Copolymers ». *Materials Letters* 62 (17-18): 3152-55. https://doi.org/10.1016/j.matlet.2008.02.008.

Caron, Vincent, Yun Hu, Lidia Tajber, Andrea Erxleben, Owen I. Corrigan, Patrick McArdle, et Anne Marie Healy. 2013. « Amorphous Solid Dispersions of Sulfonamide/Soluplus® and Sulfonamide/PVP Prepared by Ball Milling ». *AAPS PharmSciTech* 14 (1): 464-74. https://doi.org/10.1208/s12249-013-9931-7.

Choudhary, Ankush, Avtar C. Rana, Geeta Aggarwal, Virender Kumar, et Foziyah Zakir. 2012. « Development and Characterization of an Atorvastatin Solid Dispersion Formulation Using

Skimmed Milk for Improved Oral Bioavailability ». *Acta Pharmaceutica Sinica B* 2 (4): 421-28. https://doi.org/10.1016/j.apsb.2012.05.002.

Christensen, Niels Peter Aae, Bernard Van Eerdenbrugh, Kaho Kwok, Lynne S. Taylor, Andrew D. Bond, Thomas Rades, Jukka Rantanen, et Claus Cornett. 2013. « Rapid Insight into Heating-Induced Phase Transformations in the Solid State of the Calcium Salt of Atorvastatin Using Multivariate Data Analysis ». *Pharmaceutical Research* 30 (3): 826-35. https://doi.org/10.1007/s11095-012-0923-1.

Clevers, S., F. Simon, V. Dupray, et G. Coquerel. 2013. « Temperature Resolved Second Harmonic Generation to Probe the Structural Purity of M-Hydroxybenzoic Acid ». *Journal of Thermal Analysis and Calorimetry* 112 (1): 271-77. https://doi.org/10.1007/s10973-012-2763-y.

Colhoun H.M., D.J. Betteridge, P.N. Durrington, G.A. Hitman, H.A. Neil, S.J. Livingstone, M.J. Thomason, M.I. Mackness, V. Charlton-Menys, J.H. Fuller, Primary prevention of cardiovascular disease with atorvastatin in type 2 diabetes in the Collaborative Atorvastatin Diabetes Study (CARDS): multicentre randomised placebocontrolled trial, *Lancet* 364 (2004) 685–696.

Desager, Jean-Pierre, et Yves Horsmans. 1996. « Clinical Pharmacokinetics of 3-Hydroxy-3-Methylglutaryl-Coenzyme A Reductase Inhibitors »: *Clinical Pharmacokinetics* 31 (5): 348-71. https://doi.org/10.2165/00003088-199631050-00003.

Dohrn, S.; Luebbert, C.; Lehmkemper, K.; Kyeremateng, S. O.; Degenhardt, M.; Sadowski, G., Solvent influence on the phase behavior and glass transition of Amorphous Solid Dispersions. *Eur. J. Pharm. Biopharm.* **2021,** *158*, 132-142.

Dohrn, S.; Reimer, P.; Luebbert, C.; Lehmkemper, K.; Kyeremateng, S. O.; Degenhardt, M.; Sadowski, G., Thermodynamic Modeling of Solvent-Impact on Phase Separation in Amorphous Solid Dispersions during Drying. *Mol Pharm* **2020,** *17* (7), 2721-2733.

Dong, Wenxiang, Xitong Su, Meng Xu, Mingming Hu, Yinghua Sun, et Peng Zhang. 2018. « Preparation, Characterization, and in Vitro/Vivo Evaluation of Polymer-Assisting Formulation of Atorvastatin Calcium Based on Solid Dispersion Technique ». *Asian Journal of Pharmaceutical Sciences* 13 (6): 546-54. https://doi.org/10.1016/j.ajps.2018.08.010.

Galland, Arnaud, Valerie Dupray, Benjamin Berton, Sandrine Morin-Grognet, Morgane Sanselme, Hassan Atmani, et Gérard Coquerel. 2009. « Spotting Conglomerates by Second Harmonic Generation ». *Crystal Growth & Design* 9 (6): 2713-18. https://doi.org/10.1021/cg801356m.

Gordon, J M, G B Rouse, J H Gibbs, et W M Risen Jr. 2014. « The Composition Dependence of Glass Transition Properties » 66 (11): 7.

Ha, Eun-Sol, In-hwan Baek, Wonkyung Cho, Sung-Joo Hwang, et Min-Soo Kim. 2014. « Preparation and Evaluation of Solid Dispersion of Atorvastatin Calcium with Soluplus® by Spray Drying Technique ». *Chemical and Pharmaceutical Bulletin* 62 (6): 545-51. https://doi.org/10.1248/cpb.c14-00030.

Hu, L, D Gu, Q Hu, Y Shi, et N Gao. 2014. « Investigation of Solid Dispersion of Atorvastatin Calcium in Polyethylene Glycol 6000 and Polyvinylpyrrolidone ». *Tropical Journal of Pharmaceutical Research* 13 (6): 835. https://doi.org/10.4314/tjpr.v13i6.2.

Kalogeras, Ioannis M. 2010. « Description and Molecular Interpretations of Anomalous Compositional Dependences of the Glass Transition Temperatures in Binary Organic Mixtures ». *Thermochimica Acta*, 12.

Kasim, Nehal A, Marc Whitehouse, Chandrasekharan Ramachandran, Marival Bermejo, Hans Lennerna, Salomon A Stavchansky, Kamal K Midha, Vinod P Shah, et Gordon L Amidon. s. d. « Molecular Properties of WHO Essential Drugs and Provisional Biopharmaceutical Classification », 12.

Kim, Jeong-Soo, Min-Soo Kim, Hee Jun Park, Shun-Ji Jin, Sibeum Lee, et Sung-Joo Hwang. 2008. « Physicochemical Properties and Oral Bioavailability of Amorphous Atorvastatin Hemi-Calcium Using Spray-Drying and SAS Process ». *International Journal of Pharmaceutics* 359 (1-2): 211-19. https://doi.org/10.1016/j.ijpharm.2008.04.006.

Kumar, Nagendra, Sundeep Chaurasia, Ravi R. Patel, Gayasuddin Khan, Vikas Kumar, et Brahmeshwar Mishra. 2017. « Atorvastatin Calcium Encapsulated Eudragit Nanoparticles with Enhanced Oral Bioavailability, Safety and Efficacy Profile ». *Pharmaceutical Development and Technology* 22 (2): 156-67. https://doi.org/10.3109/10837450.2015.1108983.

Kwei, T. K. 1984. « The Effect of Hydrogen Bonding on the Glass Transition Temperatures of Polymer Mixtures ». *Journal of Polymer Science: Polymer Letters Edition* 22 (6): 307-13. https://doi.org/10.1002/pol.1984.130220603.

Lau, Yvonne Y., Hideaki Okochi, Yong Huang, et Leslie Z. Benet. 2006. « Pharmacokinetics of atorvastatin and its hydroxy metabolites in rats and the effects of concomitant rifampicin single doses: relevance of first-pass effect from hepatic uptake transporters, and intestinal and hepatic metabolism ». *Drug Metabolism and Disposition* 34 (7): 1175-81. https://doi.org/10.1124/dmd.105.009076.

Law, Devalina, Eric A. Schmitt, Kennan C. Marsh, Elizabeth A. Everitt, Weili Wang, James J. Fort, Steven L. Krill, et Yihong Qiu. 2004. « Ritonavir–PEG 8000Amorphous Solid Dispersions: In Vitro and In Vivo Evaluations ». *Journal of Pharmaceutical Sciences* 93 (3): 563-70. https://doi.org/10.1002/jps.10566.

Lemsi, Malek, Haykel Galai, Mohamed Radhouan Louhaichi, Hatem Fessi, et Rafik Kalfat. 2017. « Amorphization of Atorvastatin Calcium by Mechanical Process: Characterization and Stabilization Within Polymeric Matrix ». *Journal of Pharmaceutical Innovation* 12 (3): 216-25. https://doi.org/10.1007/s12247-017-9282-0.

Lipitor. Package Insert, Pfizer Ireland Pharmaceuticals, Dublin, Ireland. Parke Davis, Division of Pfizer Inc, New York; 2009.

Löbenberg, Raimar, et Gordon L Amidon. 2000. « Modern Bioavailability, Bioequivalence and Biopharmaceutics Classi®cation System. New Scienti®c Approaches to International Regulatory Standards ». *European Journal of Pharmaceutics and Biopharmaceutics*, 50 (2000) 3-12.

Maurya, Durgaprasad, Veena Belgamwar, et Avinash Tekade. 2010. « Microwave Induced Solubility Enhancement of Poorly Water Soluble Atorvastatin Calcium ». *Journal of Pharmacy and Pharmacology* 62 (11): 1599-1606. https://doi.org/10.1111/j.2042-7158.2010.01187.x.

Newa, M, K Bhandari, D Li, T Kwon, J Kim, B Yoo, J Woo, W Lyoo, C Yong, et H Choi. 2007. « Preparation, Characterization and in Vivo Evaluation of Ibuprofen Binary Solid Dispersions with Poloxamer 188 ». *International Journal of Pharmaceutics* 343 (1-2): 228-37. https://doi.org/10.1016/j.ijpharm.2007.05.031.

Newman, Ann, et George Zografi. 2020. « What We Need to Know about Solid-State Isothermal Crystallization of Organic Molecules from the Amorphous State below the Glass Transition Temperature ». *Mol. Pharmaceutics*, 2020, 17, 1761−1777. https://dx.doi.org/10.1021/acs.molpharmaceut.0c00181.

Pasceri, Vincenzo, Giuseppe Patti, Annunziata Nusca, Christian Pristipino, Giuseppe Richichi, et Germano Di Sciascio. s. d. « Randomized Trial of Atorvastatin for Reduction of Myocardial Damage During Coronary Intervention », 6.

Rumondor, Alfred C. F., Igor Ivanisevic, Simon Bates, David E. Alonzo, et Lynne S. Taylor. 2009. « Evaluation of Drug-Polymer Miscibility in Amorphous Solid Dispersion Systems ». *Pharmaceutical Research* 26 (11): 2523-34. https://doi.org/10.1007/s11095-009-9970-7.

S. K. Kurtz and T. T. Perry, "A Powder Technique for the Evaluation of Nonlinear Optical Materials," J. Appl. Phys., vol. 39, no. 8, pp. 3798–3813, 1968.

Shamsuddin, Mohammad Fazil, ShahidH Ansari, et Javed Ali. 2016. « Atorvastatin Solid Dispersion for Bioavailability Enhancement ». *Journal of Advanced Pharmaceutical Technology and Research* 7 (1): 22. https://doi.org/10.4103/2231-4040.169873.

Shete, Ganesh, Vibha Puri, Lokesh Kumar, et Arvind K. Bansal. 2010. « Solid State Characterization of Commercial Crystalline and Amorphous Atorvastatin Calcium Samples ». *AAPS PharmSciTech* 11 (2): 598-609. https://doi.org/10.1208/s12249-010-9419-7.

Sinha, Shilpi, Mushir Ali, Sanjula Baboota, Alka Ahuja, Anil Kumar, et Javed Ali. s. d. « Solid Dispersion as an Approach for Bioavailability Enhancement of Poorly Water-Soluble Drug Ritonavir », 11.

Tizaoui, Chaima, Haykel Galai, Maria Barrio, Simon Clevers, Nicolas Couvrat, Valérie Dupray, Gérard Coquerel, Josep-Lluis Tamarit, et Ivo B. Rietveld. 2020. « Does the Trihydrate of Atorvastatin Calcium Possess a Melting Point? » *European Journal of Pharmaceutical Sciences* 148 (mai): 105334. https://doi.org/10.1016/j.ejps.2020.105334.

Taksande J.B., Lade S.N., Trivedi R.V., Mahore J.G., Umekar M.J.,Effect of hydrophilic polymer on solubility and dissolution of atorvastatin inclusion complex. *International journal of pharmaceutical and chemical sciences* 1 (2012) 374-385.

Variankaval, Narayan, Aaron S. Cote, et Michael F. Doherty. 2008. « From Form to Function: Crystallization of Active Pharmaceutical Ingredients ». *AIChE Journal* 54 (7): 1682-88. https://doi.org/10.1002/aic.11555.

Won, Dong-Han, Min-Soo Kim, Sibeum Lee, Jeong-Sook Park, et Sung-Joo Hwang. 2005. « Improved Physicochemical Characteristics of Felodipine Solid Dispersion Particles by Supercritical Anti-Solvent Precipitation Process ». *International Journal of Pharmaceutics* 301 (1-2): 199-208. https://doi.org/10.1016/j.ijpharm.2005.05.017.

Zerrouk, Naima, Chantal Chemtob, Philippe Arnaud, Siro Toscani, et Jerome Dugue. 2001. « In Vitro and in Vivo Evaluation of Carbamazepine-PEG 6000 Solid Dispersions ». *International Journal of Pharmaceutics* 225 (1-2): 49-62. https://doi.org/10.1016/S0378-5173(01)00741-4.

Zhang, Hai-Xia, Jie-Xin Wang, Zhi-Bing Zhang, Yuan Le, Zhi-Gang Shen, et Jian-Feng Chen. 2009. « Micronization of Atorvastatin Calcium by Antisolvent Precipitation Process ». *International Journal of Pharmaceutics* 374 (1-2): 106-13. https://doi.org/10.1016/j.ijpharm.2009.02.015.

Zhen-Hai Zhang, Jian-Ping Zhou, Hui-Xia Ly, et al. 2012. « Preparation, Physicochemical Characteristics and Bioavailability Studies of an Atorvastatin Hydroxypropyl-ß-Cyclodextrin Complex », *Pharmazie* 67: 46–53 (2012). https://doi.org/10.1691/ph.2012.1082.

Graphical Abstract

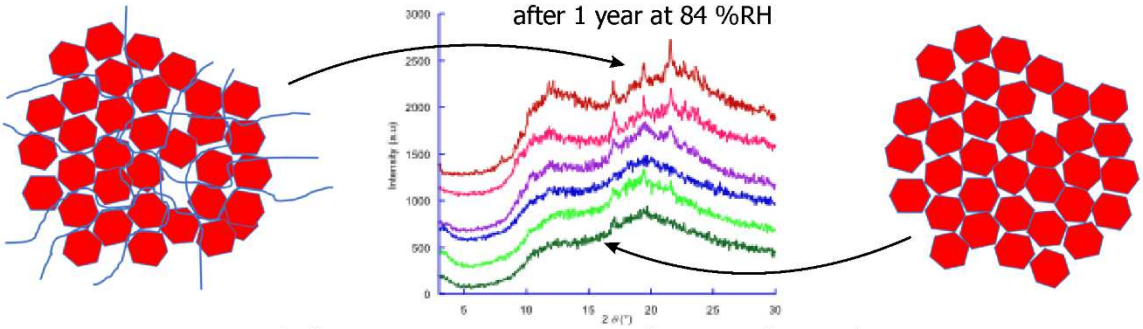

higher persistency against crystallisation without polymer